ProteinAligner: A Multi-modal Pretraining Framework for Protein Foundation Models

Li Zhang[1, *], **Han Guo**[1, *], **Leah Schaffer**[2], **Young Su Ko**[3], **Digvijay Singh**[4], **Hamid Rahmani**[5], **Danielle Grotjahn**[5], **Elizabeth Villa**[4,6], **Michael Gilson**[7], **Wei Wang**[3,8], **Trey Ideker**[2,9], **Eric Xing**[10,11], **and Pengtao Xie**[1,2,11] ✉

[1]Department of Electrical and Computer Engineering, University of California San Diego, La Jolla, CA 92093, USA
[2]Department of Medicine, University of California San Diego, La Jolla, CA 92093, USA
[3]Department of Chemistry and Biochemistry, University of California San Diego, La Jolla, CA 92093, USA
[4]School of Biological Sciences, University of California San Diego, La Jolla, CA 92093, USA
[5]Department of Integrative Structural and Computational Biology, The Scripps Research Institute, La Jolla, CA 92037, USA
[6]Howard Hughes Medical Institute, University of California San Diego, La Jolla, CA 92093, USA
[7]Skaggs School of Pharmacy and Pharmaceutical Sciences, University of California San Diego, La Jolla, CA 92093, USA
[8]Department of Cellular and Molecular Medicine, University of California San Diego, La Jolla, CA 92093, USA
[9]Department of Bioengineering, University of California San Diego, La Jolla, CA 92093, USA
[10]Machine Learning Department, Carnegie Mellon University, Pittsburgh, PA 15213, USA
[11]Mohamed bin Zayed University of Artificial Intelligence, Masdar City, Abu Dhabi, UAE

Protein foundation models, particularly protein language models, have demonstrated strong success in learning meaningful representations of proteins using transformer architectures pretrained on large-scale protein datasets with self-supervised learning. These representations have been highly effective for downstream tasks such as predicting protein functions and properties. However, most current protein foundation models focus on pretraining with amino acid sequences, often neglecting additional modalities like protein structures and related literature, both of which provide valuable insights. To address this gap, we propose a multi-modal pretraining approach that integrates three key modalities - protein sequences, structures, and literature text. In our framework, the protein sequence modality serves as the anchor, with the other two modalities aligned to it, enhancing the model's capacity to capture more comprehensive protein information. ProteinAligner outperformed state-of-the-art protein foundation models in predicting protein functions and properties across diverse downstream tasks.

Protein foundation model, multi-modal learning, protein function prediction, protein property prediction

Correspondence: ***p1xie@ucsd.edu***

**** Equal contribution***

Introduction

Proteins play a fundamental role in virtually all biological processes. Understanding their functions and properties is central to advancing fields such as drug discovery (1), diagnostics (2), and biotechnology (3). Recent advances in artificial intelligence, particularly in transformer-based models (4), have led to the development of protein foundation models capable of learning rich representations from large-scale protein datasets (5–11). These models, particularly protein language models (PLMs) (5–7, 10, 11), have shown remarkable success in performing various downstream tasks such as protein function prediction (12, 13), property prediction (14, 15), structure prediction (16, 17), and protein design (18, 19).

Despite these successes, current PLMs predominantly focus on amino acid sequences while overlooking the wealth of complementary information available in other modalities. Protein structures, for example, provide critical three-dimensional information that is essential for understanding how proteins fold and interact with other molecules, directly influencing their biological functions (20). The spatial arrangement of amino acids, which governs interactions such as binding affinities and functional sites, cannot be readily inferred from sequence data alone (21, 22), making the integration of structural data crucial for a more comprehensive understanding of protein behavior. Similarly, the vast amount of biological literature contains experimentally validated insights into protein mechanisms, behavior, and interactions that are often context-specific and difficult to infer from sequences or structures alone (23, 24). Literature captures critical information about post-translational modifications, protein dynamics in various environments, and interaction networks - details accumulated from years of experimental studies. By incorporating these additional modalities - protein structures and related literature - protein foundation models can move beyond sequence prediction to a more robust, context-aware understanding of protein biology. This multi-modal integration has the potential to greatly enhance the representational power of these models, enabling more accurate predictions of protein functions and behaviors in diverse biological scenarios. While some studies have explored the use of two modalities, such as protein sequence and text (24–26) or protein structure and sequence (8, 9, 27), the simultaneous integration of three modalities for pretraining protein foundation models remains underexplored.

To address this gap, we introduce ProteinAligner, a multi-modal pretraining framework that combines protein sequences, structures, and literature text. Our framework aligns these modalities with the protein sequence as the anchor, enabling the model to learn richer and more comprehensive representations of proteins. By integrating diverse protein-related data, ProteinAligner improves the model's ability to capture intricate biological phenomena, paving the way for more accurate predictions of protein functions and properties. ProteinAligner utilizes three specialized encoders - a sequence encoder, a structure encoder, and a text encoder - to learn representations for each modality. These distinct representations are projected into a shared latent space, enabling direct comparison across modalities. By employing a contrastive alignment strategy (28), ProteinAligner uses protein sequences as the anchor to align corresponding structures and textual descriptions, encouraging similar representations for the same protein and dissimilar representations for different proteins. This approach not only maximizes data utilization by allowing pretraining on incomplete modality data but also captures the comprehensive biological insights provided by each modality. Recently, another independent study (29) also explored learning protein representations across three modalities. Their work and ours were developed independently, with approaches and experiments conceived separately.

ProteinAligner demonstrated superior performance compared to state-of-the-art baselines across various downstream prediction tasks, including detecting type I anti-CRISPR activities, predicting pathogenic missense variants, predicting protein thermostability, identifying potent bioactive peptides, and estimating the minimum inhibitory concentration of antimicrobial peptides.

Results

ProteinAligner overview. ProteinAligner is a multi-modal foundation model for protein representation learning, integrating three distinct modalities: amino acid (AA) sequences, 3D structures, and textual descriptions of proteins. ProteinAligner contains three encoders - a protein sequence encoder, a protein structure encoder, and a text encoder - each dedicated to learning representations for its corresponding modality (Fig. 1a). The protein sequence encoder is a protein language model that uses the transformer architecture (4) to extract a representation for the input AA sequence. It represents each AA as a token and employs self-attention (4) to capture long-range dependencies among AAs. The protein structure encoder utilizes Geometric Vector Perceptron Graph Neural Network (GVP-GNN) (30) layers for geometric representation learning of the input protein structure, followed by transformer layers that capture long-range interactions between atomic coordinates. The text encoder employs a transformer architecture, utilizing self-attention to capture long-range dependencies between language tokens. Specifically, we employed ESM (5), a leading protein language model, as the protein sequence encoder, and ESM-IF1 (9) as the protein structure encoder. ESM consists of 33 transformer layers and 650 million parameters, pretrained on 65 million protein sequences. ESM-IF1 features 20 layers and 124 million parameters, pretrained on 12 million computed protein structures and 16,000 experimentally verified structures. The text encoder includes eight transformer layers with a total of 78 million parameters. ProteinAligner uses modality-specific linear projection modules to map the representations extracted by different encoders into a shared latent space with matching dimensions, ensuring that representations from different modalities are directly comparable. ProteinAligner consists of 867 million model parameters in total.

ProteinAligner performs joint pretraining of the three encoders by leveraging a modality alignment strategy, using protein sequences as the anchor modality to align the other two modalities (Fig. 1a). Specifically, given a protein sequence and a protein structure, if they correspond to the same protein, ProteinAligner encourages their representations to be similar, and dissimilar otherwise. The same principle applies for protein text and protein sequences, with representations aligned if they refer to the same protein and separated if not. This alignment is accomplished by minimizing contrastive losses (28, 31) defined on the representations of sequence-structure pairs and sequence-text pairs. ProteinAligner does not require all three modalities to be present simultaneously for each protein in the pretraining data. The alignment can be performed as long as the protein sequence and at least one additional modality - either structure or text - are available. We chose protein sequences as the anchor for alignment because they are the most prevalent data modality in protein databases; nearly every protein has an associated amino acid sequence, whereas information on structures or textual descriptions is often incomplete. By using sequences as the anchor, we can maximize data utilization, ensuring the inclusion of as many proteins as possible in the alignment process. With pretrained encoders in place, they can be fine-tuned on task-specific data to handle a variety of downstream tasks. During this process, the encoders are integrated with task-specific modules, creating models that are customized for specific prediction tasks.

We curated a large-scale pretraining dataset for ProteinAligner by integrating data from the UniProtKB/Swiss-Prot (32) and RCSB PDB (33) databases. The dataset consists of 290,480 proteins, each with an amino acid sequence and a corresponding textual description. 133,726 of them are also associated with protein structures. In total, the dataset contains 133,726 sequence-structure pairs and 290,480 sequence-text pairs. The textual descriptions provide information about the proteins' functions. Both the structures and the functional descriptions were experimentally validated and reviewed by domain experts. Fig. 1b shows the distribution of protein taxonomy, functions, and types in the dataset.

ProteinAligner detects type I anti-CRISPR activities. We evaluated the effectiveness of ProteinAligner in detecting type I anti-CRISPR (Acr) activities. Acr proteins are produced by certain viruses, such as bacteriophages, or mobile genetic elements to inhibit the type I CRISPR-Cas

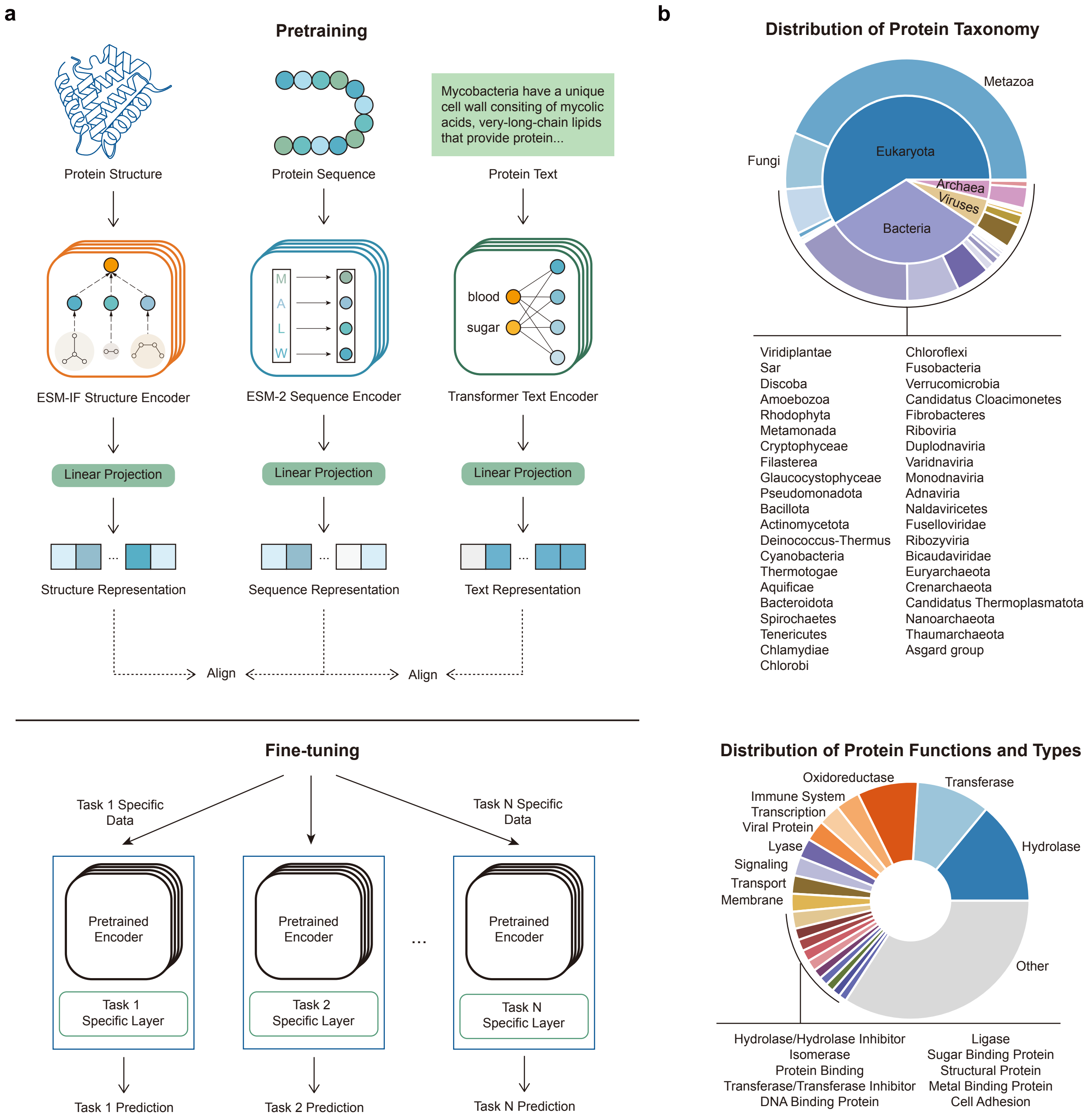

Fig. 1 | ProteinAligner facilitates multi-modal pretraining of protein foundation models by integrating diverse modalities including amino acid sequences, 3D structures, and textual data. **a**, ProteinAligner consists of three encoders: a protein sequence encoder based on ESM, a protein structure encoder based on ESM-IF1, and a transformer-based protein text encoder. These encoders learn representations for protein sequences, structures, and text, respectively. Modality-specific projection modules then transform these representations into a shared latent space, enabling direct comparison across modalities. Using protein sequences as the anchor, ProteinAligner aligns the other two modalities by minimizing contrastive losses. After pretraining, the encoders can be fine-tuned with task-specific data for various downstream applications. **b**, Our curated pretraining data for ProteinAligner spans a diverse range of proteins from various taxonomic groups, functions, and types. The upper chart displays the distribution of protein taxonomy, with the inner ring representing superkingdoms and the outer ring representing kingdoms. The lower chart illustrates the distribution of protein functions and types.

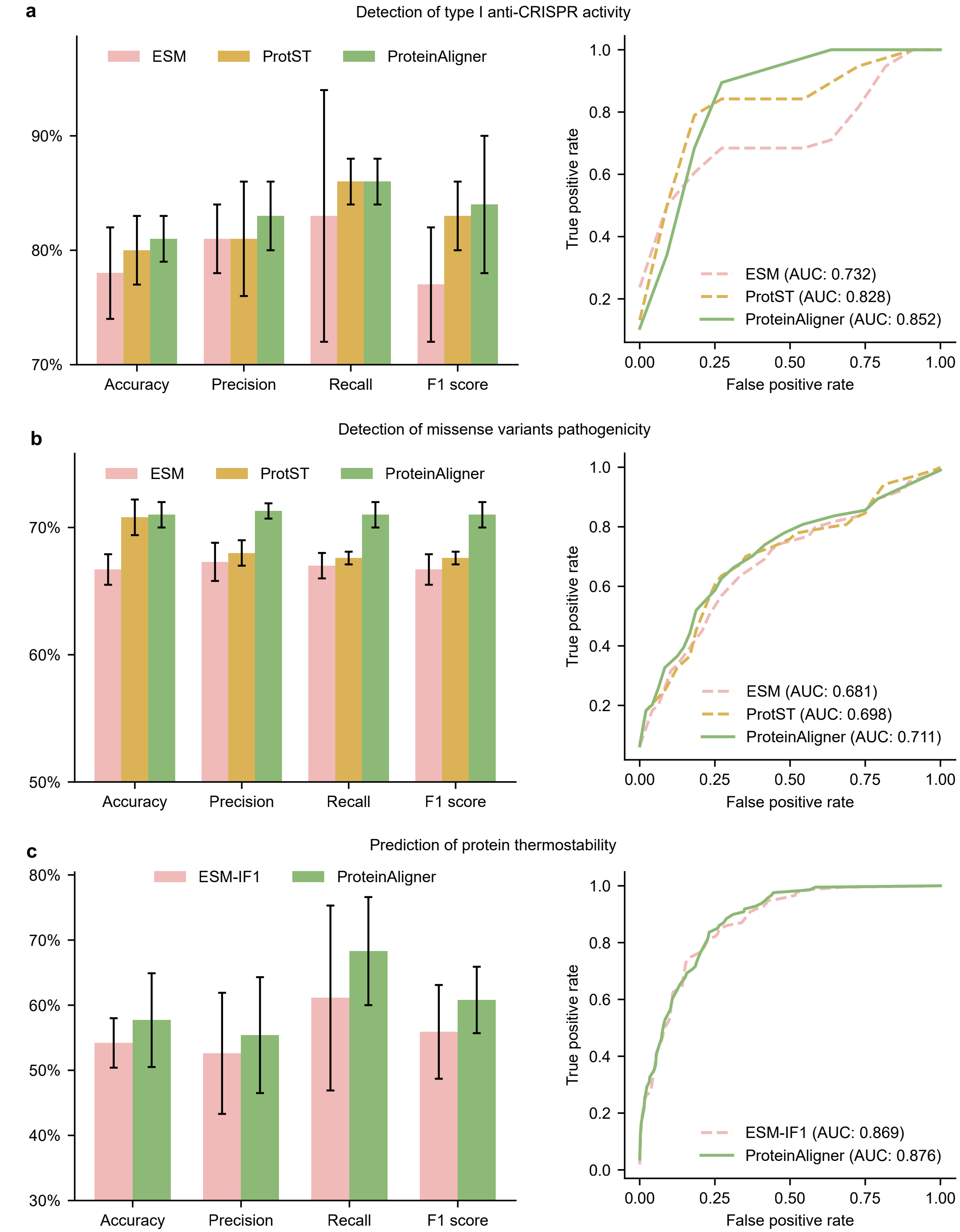

Fig. 2 | ProteinAligner outperforms state-of-the-art protein foundation models in various downstream tasks. a-b, ProteinAligner's sequence encoder outperforms ESM and ProST in detecting type I anti-CRISPR activity (**a**) and pathogenic missense variants (**b**), achieving higher accuracy, F1 scores (which balance precision and recall), and area under the ROC curve (AUC). **c**, ProteinAligner's structure encoder outperforms ESM-IF1 in predicting protein thermostability.

immune system in bacteria and archaea (34). The CRISPR-Cas system functions as an adaptive immune mechanism in these microorganisms, recognizing and cleaving foreign DNA from viral invaders. In type I systems, which involve multi-subunit Cas proteins, Acr proteins disrupt this defense by preventing Cas proteins from binding to target DNA or carrying out their cleavage functions. Understanding and detecting these Acr activities is crucial for controlling CRISPR-Cas systems in genetic engineering and leveraging bacteriophages to combat antimicrobial resistance.

Given the amino acid sequences of an Arc protein and a set of Cas proteins from a CRISPR-Cas system, we employed ProteinAligner's pretrained sequence encoder to extract representation vectors for each protein. These vectors were then input into a convolutional neural network (CNN) based classification module to predict whether the Arc protein could inhibit the CRISPR-Cas system. We utilized the Acr-CRISPR-Cas inhibition dataset (34) for experiments, which comprises 227 pairs of Acr proteins and CRISPR-Cas systems, including 132 experimentally verified positive pairs (Acr inhibits CRISPR-Cas) and 95 negative pairs (Acr does not inhibit CRISPR-Cas). The dataset was randomly split into training and test sets in an 8:2 ratio. We compared ProteinAligner to ESM (5), a protein language model pretrained on protein sequences, and ProtST (24), which builds on ESM by incorporating contrastive pretraining between protein sequences and text. We used area under the ROC curve (AUC), accuracy, precision, recall, and F1 score as evaluation metrics.

ProteinAligner demonstrated significantly better performance across all metrics in detecting type I anti-CRISPR activity compared to ESM (Fig. 2a). For instance, ProteinAligner achieved an AUC of 0.852, substantially surpassing ESM's AUC of 0.732. Similarly, ProteinAligner's F1 score of 0.84 was considerably higher than ESM's F1 score of 0.77. Moreover, ProteinAligner achieved superior performance compared to ProtST (Fig. 2a).

ProteinAligner predicts pathogenic missense variants. Pathogenic missense variants refer to specific types of genetic mutations where a single nucleotide change in a DNA sequence results in the substitution of one amino acid for another in the corresponding protein (35). This change can disrupt the protein's normal function, potentially leading to diseases or disorders. In the context of pathogenicity, these variants are considered harmful because they alter the protein's structure or function in a way that impairs biological processes. Depending on the protein's role, this can lead to a variety of outcomes, from minor effects to severe genetic disorders, such as cystic fibrosis, sickle cell disease, or certain forms of cancer. Identifying and characterizing pathogenic missense variants is crucial in genetic research and clinical diagnostics for understanding inherited diseases and developing targeted treatments.

The inputs for this task are two protein sequences: the wildtype sequence (before mutation) and the mutant sequence (after mutation). We employed the sequence encoder in ProteinAligner to extract representation vectors for both proteins. These vectors were then concatenated and passed through a multi-layer perceptron to predict whether the mutant protein is pathogenic. We used 200 labeled examples from the VariPred (36) dataset, with 100 examples allocated for training and the remaining 100 for testing. ProteinAligner outperformed both ESM and ProtST (Fig. 2b). For example, it achieved an F1 score of 0.71 compared to 0.667 for ESM and 0.676 for ProtST.

ProteinAligner predicts protein thermostability. Protein thermostability refers to a protein's ability to maintain its structure and function when exposed to elevated temperatures (37). This characteristic is critical because proteins typically lose their functional shape, or denature, at high temperatures, rendering them ineffective. Thermostability is an important factor in various biological processes and industrial applications. For instance, enzymes with high thermostability are essential in industries such as biotechnology and pharmaceuticals, where reactions often require high temperatures for optimal efficiency. Predicting protein thermostability allows researchers to design or engineer proteins that can withstand challenging conditions, improving their functionality and longevity. Additionally, thermostable proteins are valuable in drug design, as they tend to have better shelf lives and performance under physiological conditions. Accurate predictions of thermostability are crucial for advancing protein engineering and enhancing the reliability of proteins in various applications.

Unlike the previous two tasks, this task takes the 3D structures of proteins, specifically their atomic coordinates, as input. The 3D structure of each protein was processed through ProteinAligner's structure encoder, generating a representation vector. This vector was then passed through a multi-layer perceptron to predict the protein's thermostability class. We employed the HP-S^{2}C5 dataset (38), which comprises 1,040 proteins spanning five thermostability classes: Hyperthermophilic (above 75°C), Thermophilic (45-75°C), Mesophilic (25-45°C), Psychrophilic (5–25°C), and Cryophilic (−20–5°C). 936 proteins were used for training and 104 for testing. We compared ProteinAligner with ESM-IF1 (9), a protein structure encoder pretrained on both protein structures and sequences. ProteinAligner remarkably outperformed ESM-IF1 (Fig. 2c), achieving an F1 score of 0.608 compared to 0.559, and an accuracy of 0.577 compared to 0.542.

ProteinAligner identifies potent bioactive peptides. Bioactive peptides are short chains of amino acids with specific biological activities (39). They play critical roles in regulating physiological processes, including immune

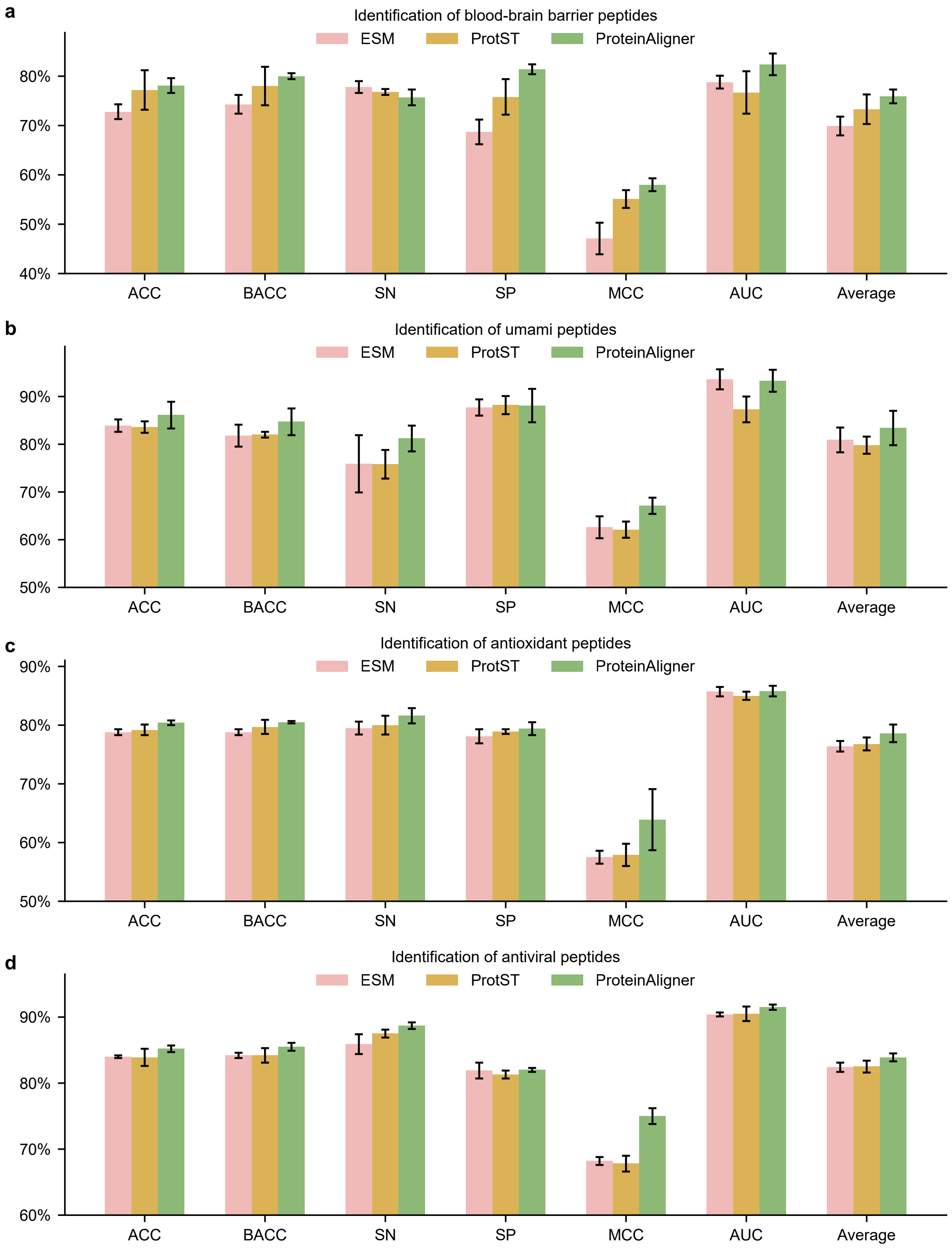

Fig. 3 | ProteinAligner surpasses ESM and ProtST in identifying potent bioactive peptides. It demonstrated superior performance in predicting blood-brain barrier penetration (**a**), umami taste induction (**b**), antioxidant activity (**c**), and antiviral properties (**d**). Model performance was evaluated using accuracy (ACC), balanced accuracy (BACC), sensitivity (SN), specificity (SP), Matthews correlation coefficient (MCC), and the area under the ROC curve (AUC).

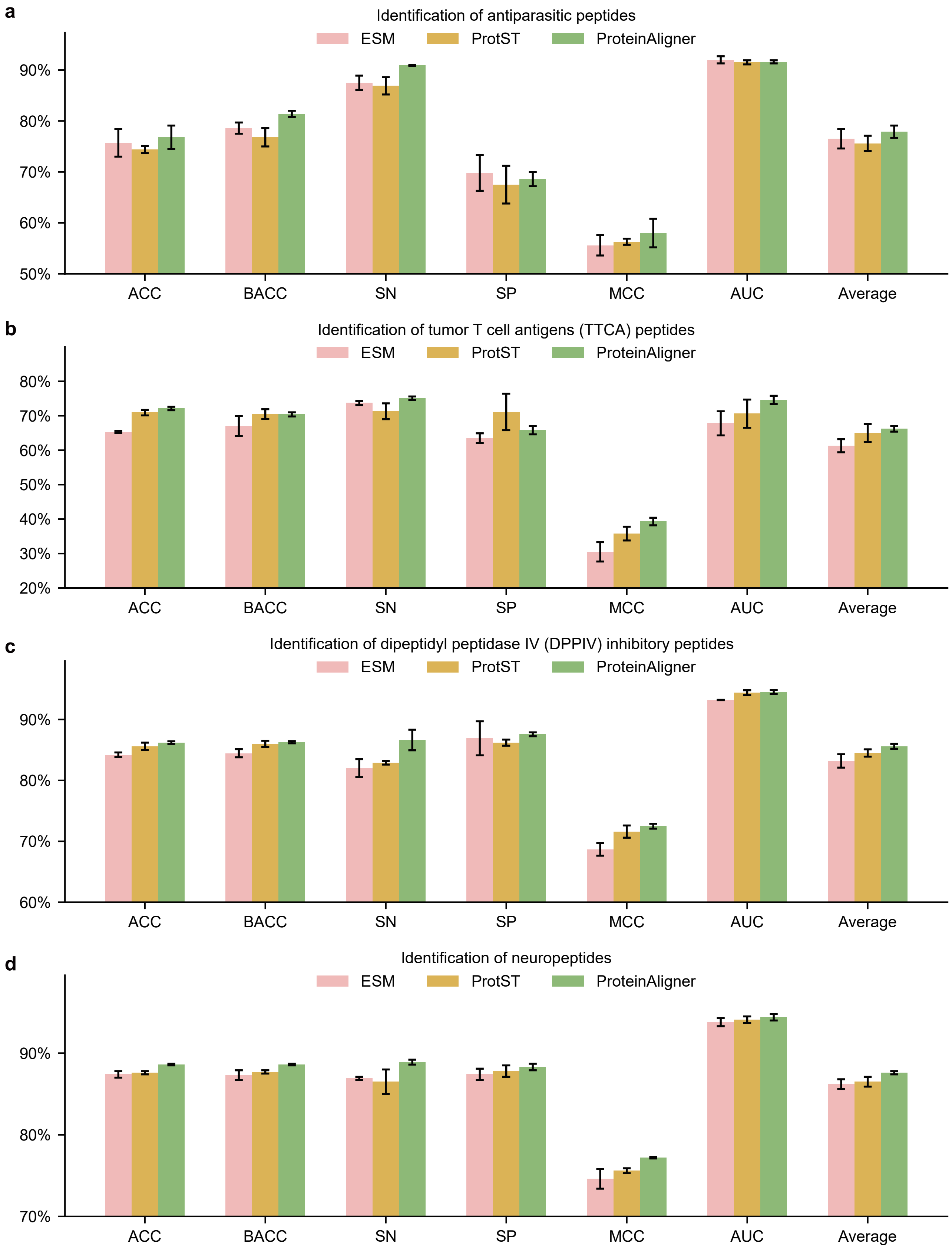

Fig. 4 | ProteinAligner outperforms ESM and ProtST in identifying potent bioactive peptides. It achieved superior performance in predicting antiparasitic effects (**a**), T-cell immune response induction (**b**), inhibition of dipeptidyl peptidase IV (DPP-IV) (**c**), and modulation of brain activity (**d**). Model performance was assessed using accuracy (ACC), balanced accuracy (BACC), sensitivity (SN), specificity (SP), Matthews correlation coefficient (MCC), and the area under the ROC curve (AUC).

function, metabolism, and cardiovascular health. Identifying bioactive peptides is important because they offer significant potential for developing new therapeutic agents and functional foods. These peptides can serve as natural, targeted treatments with fewer side effects compared to traditional drugs, and their discovery can lead to advancements in both medical applications and nutrition, benefiting public health and disease prevention efforts.

Given the amino acid sequence of a peptide, we employed ProteinAligner's protein sequence encoder to extract a representation vector, which was subsequently input into a convolutional neural network (CNN)-based classification head to predict whether the peptide has a specific bioactivity. We examined eight distinct bioactivities, including blood-brain barrier penetration (40), umami taste induction (41), antioxidant activity (42), antiviral properties (43), antiparasitic effects (44), T-cell immune response induction (45), inhibition of dipeptidyl peptidase IV (DPP-IV) (46), and modulation of brain activity (47). Given that a peptide can exhibit multiple bioactivities concurrently, we approached each bioactivity prediction as a binary classification task, avoiding the use of a multi-class model that would assign the peptide to a single category. Separate datasets were used for each bioactivity (Methods). The evaluation metrics for this task included accuracy (ACC), balanced accuracy (BACC) (48), sensitivity (SN), specificity (SP), Matthews correlation coefficient (MCC) (49), and the area under the ROC curve (AUC).

ProteinAligner consistently surpassed ESM and ProtST across all eight evaluated tasks (Figs. 3 and 4). For example, in predicting blood-brain barrier penetration, ProteinAligner achieved an AUC of 0.824, outperforming both ESM (0.788) and ProtST (0.767). Similarly, in predicting T-cell immune response induction, ProteinAligner reached an AUC of 0.746, exceeding the performance of ESM (0.678) and ProtST (0.706).

ProteinAligner predicts the minimum inhibitory concentration (MIC) of antimicrobial peptides. Antimicrobial peptides (AMPs) are short chains of amino acids that serve as a crucial part of the innate immune response in many organisms, exhibiting broad-spectrum activity against bacteria, viruses, fungi, and even cancer cells (50). They function by disrupting microbial membranes, leading to cell death, and are considered potential alternatives to conventional antibiotics, especially in the face of rising antibiotic resistance. The minimum inhibitory concentration (MIC) is the lowest concentration of an antimicrobial agent, such as an AMP, that prevents visible microbial growth. Accurately predicting the MIC values of AMPs is essential as it allows for the optimization of peptide design for therapeutic use, minimizes potential toxicity, and helps in the early-stage screening of effective peptides before in vitro or in vivo testing. This predictive capability is vital for accelerating the development of AMPs as a novel class of antimicrobial agents in clinical applications.

Given the amino acid sequence of a peptide, we applied ProteinAligner's protein sequence encoder to extract a representation vector, which was then fed into a multi-layer perceptron-based regression module to predict the MIC of the peptide against a specific pathogen. We focused on Escherichia coli (E. coli), a gram-negative bacterium. We utilized the dataset from (51), comprising 3,695 training and 924 testing examples. Mean squared error was used as the evaluation metric. ProteinAligner achieved lower prediction error compared to ESM and ProtST (Extended Data Fig. 1).

Discussion

ProteinAligner demonstrates superior performance compared to models like ESM and ProtST by employing a multi-modal approach that integrates sequences, structures, and textual information, offering a more comprehensive understanding of proteins (Figs. 2a, 2b, 3, 4, and Extended Data Fig.1). While ESM focuses on learning from amino acid sequences, ProteinAligner incorporates protein structures, which provide critical insights into folding, stability, and interaction dynamics that sequences alone cannot reveal. Additionally, by drawing from experimental literature, ProteinAligner captures contextual information like functional annotations and post-translational modifications, bridging gaps in sequence and structure-based models. The multi-modal alignment in a shared latent space enables ProteinAligner to generate representations that are not only sequence-based but also grounded in functional and structural knowledge, leading to more accurate predictions. Compared to ProtST, which integrates sequence and text data, ProteinAligner adds the essential dimension of protein structure, crucial for understanding spatial arrangements and physical properties. This enriched representation enables the model to better predict protein functions influenced by structural conformation, outperforming ProtST's dual-modality approach. Additionally, ProteinAligner surpasses ESM-IF1 (Fig. 2c), which combines sequences and structures, by incorporating textual descriptions that provide further context from experimental literature. ProteinAligner's contrastive alignment strategy ensures that the representations from sequences, structures, and text are effectively integrated, enhancing its predictive capacity across different tasks. This holistic approach equips ProteinAligner to excel in both sequence- and structure-based predictions, offering a more nuanced understanding of protein properties and delivering superior performance across a range of biological applications.

ProteinAligner's ability to perform a wide range of prediction tasks presents promising applications across biology, drug discovery, and medicine. In drug discovery, ProteinAligner's accurate identification of bioactive peptides, such as DPP-IV inhibitors (Fig. 4c), is particularly relevant for developing treatments for metabolic disorders like diabetes. Its capability to predict antimicrobial peptide properties, such as minimum inhibitory concentration (MIC) (Extended Data Fig. 1), is critical for advancing new antimicrobial therapies, especially in addressing the challenge of antibiotic-resistant pathogens. This has important implications for the global fight against antimicrobial resistance. The model's ability to detect type I anti-CRISPR activities supports the design of more efficient and precise CRISPR-based tools for both research and therapeutic applications (Fig. 2a). Anti-CRISPR systems could be used to enhance the safety of gene editing by mitigating off-target effects or enabling reversible gene modifications. In precision medicine, the prediction of pathogenic missense variants aids in the early detection and diagnosis of genetic disorders. By identifying harmful mutations that may lead to diseases, ProteinAligner can contribute to personalized treatment strategies, improving patient outcomes (Fig. 2b). Additionally, ProteinAligner's accurate prediction of protein thermostability is vital for protein engineering, biopharmaceutical development, and industrial biotechnology, where stable proteins are necessary for drug formulations and biocatalysts (Fig. 2c). Overall, ProteinAligner's diverse prediction capabilities position it as a valuable tool that can accelerate innovation in multiple fields, enabling faster therapeutic discoveries, more precise gene-editing tools, and advancements in personalized medicine and protein engineering.

Despite the advantages of ProteinAligner, the model has several limitations. One of the key challenges is the dependency on high-quality structural and textual data, which is not always available for all proteins. While ProteinAligner can perform pretraining even when only sequences and one additional modality (either structure or text) are present, the absence of full multi-modal data for many proteins can limit the model's ability to learn comprehensive representations. Additionally, ProteinAligner's reliance on contrastive loss for modality alignment may not fully capture subtle biological nuances in cases where sequence, structure, and text data are not perfectly aligned. Another limitation is the computational cost associated with training multi-modal models, especially when dealing with large-scale protein datasets that involve high-dimensional structural information and large text corpora. Finally, while ProteinAligner improves upon previous models by integrating structure, sequence, and text, it still does not account for other potentially informative modalities, such as protein-protein interactions or functional annotations from various databases, which could further enhance its predictive capabilities.

Future work on ProteinAligner could focus on several key directions to further enhance its performance and applicability. One promising area is the incorporation of additional modalities, such as protein-protein interaction networks and post-translational modifications. These additional data sources could provide deeper insights into protein behavior and interactions, leading to even more robust and comprehensive protein representations. Another direction for future work is to improve the model's ability to handle incomplete or noisy data by developing more sophisticated alignment strategies that better tolerate inconsistencies between modalities. Enhancing the interpretability of ProteinAligner's predictions is also a critical area for future research, which could involve incorporating explainability techniques to make the model's decision-making process more transparent, particularly in cases where sequence, structure, and text data converge. Lastly, expanding ProteinAligner's applications beyond protein function and property prediction - such as protein design and structure prediction - could broaden its impact across a wide range of biological and biomedical challenges.

References

1. James A Wells and Christopher L McClendon. Reaching for high-hanging fruit in drug discovery at protein–protein interfaces. *Nature*, 450(7172):1001–1009, 2007.
2. Carl AK Borrebaeck. Precision diagnostics: moving towards protein biomarker signatures of clinical utility in cancer. *Nature Reviews Cancer*, 17(3):199–204, 2017.
3. Irene Nobeli, Angelo D Favia, and Janet M Thornton. Protein promiscuity and its implications for biotechnology. *Nature biotechnology*, 27(2):157–167, 2009.
4. Ashish Vaswani, Noam Shazeer, Niki Parmar, Jakob Uszkoreit, Llion Jones, Aidan N Gomez, Łukasz Kaiser, and Illia Polosukhin. Attention is all you need. *Advances in neural information processing systems*, 30, 2017.
5. Alexander Rives, Joshua Meier, Tom Sercu, Siddharth Goyal, Zeming Lin, Jason Liu, Demi Guo, Myle Ott, C Lawrence Zitnick, Jerry Ma, et al. Biological structure and function emerge from scaling unsupervised learning to 250 million protein sequences. *Proceedings of the National Academy of Sciences*, 118(15):e2016239118, 2021.
6. Ahmed Elnaggar, Michael Heinzinger, Christian Dallago, Ghalia Rehawi, Yu Wang, Llion Jones, Tom Gibbs, Tamas Feher, Christoph Angerer, Martin Steinegger, et al. Prottrans: Toward understanding the language of life through self-supervised learning. *IEEE transactions on pattern analysis and machine intelligence*, 44(10):7112–7127, 2021.
7. Tristan Bepler and Bonnie Berger. Learning the protein language: Evolution, structure, and function. *Cell systems*, 12(6):654–669, 2021.
8. John Jumper, Richard Evans, Alexander Pritzel, Tim Green, Michael Figurnov, Olaf Ronneberger, Kathryn Tunyasuvunakool, Russ Bates, Augustin Žídek, Anna Potapenko, et al. Highly accurate protein structure prediction with alphafold. *Nature*, 596(7873):583–589, 2021.
9. Chloe Hsu, Robert Verkuil, Jason Liu, Zeming Lin, Brian Hie, Tom Sercu, Adam Lerer, and Alexander Rives. Learning inverse folding from millions of predicted structures. In *International Conference on Machine Learning*, pages 8946–8970. PMLR, 2022.
10. Nadav Brandes, Dan Ofer, Yam Peleg, Nadav Rappoport, and Michal Linial. Proteinbert: a universal deep-learning model of protein sequence and function. *Bioinformatics*, 38(8): 2102–2110, 2022.
11. Bo Chen, Xingyi Cheng, Pan Li, Yangli-ao Geng, Jing Gong, Shen Li, Zhilei Bei, Xu Tan, Boyan Wang, Xin Zeng, et al. xtrimopglm: unified 100b-scale pre-trained transformer for deciphering the language of protein. *arXiv preprint arXiv:2401.06199*, 2024.
12. Serbulent Unsal, Heval Atas, Muammer Albayrak, Kemal Turhan, Aybar C Acar, and Tunca Doğan. Learning functional properties of proteins with language models. *Nature Machine Intelligence*, 4(3):227–245, 2022.
13. Tianhao Yu, Haiyang Cui, Jianan Canal Li, Yunan Luo, Guangde Jiang, and Huimin Zhao. Enzyme function prediction using contrastive learning. *Science*, 379(6639):1358–1363, 2023.
14. Zachary N Flamholz, Steven J Biller, and Libusha Kelly. Large language models improve annotation of prokaryotic viral proteins. *Nature Microbiology*, 9(2):537–549, 2024.
15. Felix Teufel, José Juan Almagro Armenteros, Alexander Rosenberg Johansen, Magnús Halldór Gíslason, Silas Irby Pihl, Konstantinos D Tsirigos, Ole Winther, Søren Brunak, Gunnar von Heijne, and Henrik Nielsen. Signalp 6.0 predicts all five types of signal peptides using protein language models. *Nature biotechnology*, 40(7):1023–1025, 2022.
16. Zeming Lin, Halil Akin, Roshan Rao, Brian Hie, Zhongkai Zhu, Wenting Lu, Nikita Smetanin, Robert Verkuil, Ori Kabeli, Yaniv Shmueli, et al. Evolutionary-scale prediction of atomic-level protein structure with a language model. *Science*, 379(6637):1123–1130, 2023.
17. Ratul Chowdhury, Nazim Bouatta, Surojit Biswas, Christina Floristean, Anant Kharkar, Koushik Roy, Charlotte Rochereau, Gustaf Ahdritz, Joanna Zhang, George M Church, et al. Single-sequence protein structure prediction using a language model and deep learning. *Nature Biotechnology*, 40(11):1617–1623, 2022.
18. Ali Madani, Ben Krause, Eric R Greene, Subu Subramanian, Benjamin P Mohr, James M

Holton, Jose Luis Olmos, Caiming Xiong, Zachary Z Sun, Richard Socher, et al. Large language models generate functional protein sequences across diverse families. *Nature Biotechnology*, 41(8):1099–1106, 2023.

19. Noelia Ferruz, Steffen Schmidt, and Birte Höcker. Protgpt2 is a deep unsupervised language model for protein design. *Nature communications*, 13(1):4348, 2022.
20. Gregory A Petsko and Dagmar Ringe. *Protein structure and function*. New Science Press, 2004.
21. Qiangfeng Cliff Zhang, Donald Petrey, Lei Deng, Li Qiang, Yu Shi, Chan Aye Thu, Brygida Bisikirska, Celine Lefebvre, Domenico Accili, Tony Hunter, et al. Structure-based prediction of protein–protein interactions on a genome-wide scale. *Nature*, 490(7421):556–560, 2012.
22. Roberto Mosca, Arnaud Céol, and Patrick Aloy. Interactome3d: adding structural details to protein networks. *Nature methods*, 10(1):47–53, 2013.
23. Jinhyuk Lee, Wonjin Yoon, Sungdong Kim, Donghyeon Kim, Sunkyu Kim, Chan Ho So, and Jaewoo Kang. Biobert: a pre-trained biomedical language representation model for biomedical text mining. *Bioinformatics*, 36(4):1234–1240, 2020.
24. Minghao Xu, Xinyu Yuan, Santiago Miret, and Jian Tang. Protst: Multi-modality learning of protein sequences and biomedical texts. In *International Conference on Machine Learning*, pages 38749–38767. PMLR, 2023.
25. Ningyu Zhang, Zhen Bi, Xiaozhuan Liang, Siyuan Cheng, Haosen Hong, Shumin Deng, Jiazhang Lian, Qiang Zhang, and Huajun Chen. Ontoprotein: Protein pretraining with gene ontology embedding. *International Conference on Learning Representations*, 2022.
26. Kevin E Wu, Howard Chang, and James Zou. Proteinclip: enhancing protein language models with natural language. *bioRxiv*, pages 2024–05, 2024.
27. Varun R Shanker, Theodora UJ Bruun, Brian L Hie, and Peter S Kim. Unsupervised evolution of protein and antibody complexes with a structure-informed language model. *Science*, 385(6704):46–53, 2024.
28. Kaiming He, Haoqi Fan, Yuxin Wu, Saining Xie, and Ross Girshick. Momentum contrast for unsupervised visual representation learning. In *2020 IEEE/CVF Conference on Computer Vision and Pattern Recognition (CVPR)*, pages 9726–9735. IEEE Computer Society, 2020.
29. Jin Su, Xibin Zhou, Xuting Zhang, and Fajie Yuan. Protrek: Navigating the protein universe through tri-modal contrastive learning. *bioRxiv*, pages 2024–05, 2024.
30. Bowen Jing, Stephan Eismann, Patricia Suriana, Raphael John Lamarre Townshend, and Ron Dror. Learning from protein structure with geometric vector perceptrons. In *International Conference on Learning Representations*, 2020.
31. Aaron van den Oord, Yazhe Li, and Oriol Vinyals. Representation learning with contrastive predictive coding. *arXiv preprint arXiv:1807.03748*, 2018.
32. UniProt Consortium. Uniprot: a worldwide hub of protein knowledge. *Nucleic acids research*, 47(D1):D506–D515, 2019.
33. Stephen K Burley, Charmi Bhikadiya, Chunxiao Bi, Sebastian Bittrich, Henry Chao, Li Chen, Paul A Craig, Gregg V Crichlow, Kenneth Dalenberg, Jose M Duarte, et al. Rcsb protein data bank (rcsb. org): delivery of experimentally-determined pdb structures alongside one million computed structure models of proteins from artificial intelligence/machine learning. *Nucleic acids research*, 51(D1):D488–D508, 2023.
34. Moein Hasani, Chantel N. Trost, Nolen Timmerman, and Lingling Jin. Acrtransact: Pre-trained protein transformer models for the detection of type i anti-crispr activities. In *Proceedings of The 14th ACM Conference on Bioinformatics, Computational Biology, and Health Informatics (ACM-BCB)*, page 6, Houston, TX, USA, 2023. ACM.
35. Jun Cheng, Guido Novati, Joshua Pan, Clare Bycroft, Akvilė Žemgulytė, Taylor Applebaum, Alexander Pritzel, Lai Hong Wong, Michal Zielinski, Tobias Sargeant, et al. Accurate proteome-wide missense variant effect prediction with alphamissense. *Science*, 381 (6664):eadg7492, 2023.
36. Weining Lin, Jude Wells, Zeyuan Wang, Christine Orengo, and Andrew CR Martin. Enhancing missense variant pathogenicity prediction with protein language models using varipred. *Scientific Reports*, 14(1):8136, 2024.
37. H Pezeshgi Modarres, MR Mofrad, and AJRA Sanati-Nezhad. Protein thermostability engineering. *RSC advances*, 6(116):115252–115270, 2016.
38. Tianlong Chen, Chengyue Gong, Daniel Jesus Diaz, Xuxi Chen, Jordan Tyler Wells, Qiang Liu, Zhangyang Wang, Andrew Ellington, Alexandros Dimakis, and Adam Klivans. Hotprotein: A novel framework for protein thermostability prediction and editing. In *International Conference on Learning Representations (ICLR)*, 2023.
39. Ali Adem Bahar and Dacheng Ren. Antimicrobial peptides. *Pharmaceuticals*, 6(12):1543–1575, 2013.
40. Ruyu Dai, Wei Zhang, Wending Tang, Evelien Wynendaele, Qizhi Zhu, Yannan Bin, Bart De Spiegeleer, and Junfeng Xia. Bbppred: sequence-based prediction of blood-brain barrier peptides with feature representation learning and logistic regression. *Journal of Chemical Information and Modeling*, 61(1):525–534, 2021.
41. Yin Zhang, Chandrasekar Venkitasamy, Zhongli Pan, Wenlong Liu, and Liming Zhao. Novel umami ingredients: Umami peptides and their taste. *Journal of food science*, 82(1):16–23, 2017.
42. Tang-Bin Zou, Tai-Ping He, Hua-Bin Li, Huan-Wen Tang, and En-Qin Xia. The structure-activity relationship of the antioxidant peptides from natural proteins. *Molecules*, 21(1):72, 2016.
43. Liana Costa Pereira Vilas Boas, Marcelo Lattarulo Campos, Rhayfa Lorrayne Araujo Berlanda, Natan de Carvalho Neves, and Octávio Luiz Franco. Antiviral peptides as promising therapeutic drugs. *Cellular and Molecular Life Sciences*, 76:3525–3542, 2019.
44. Amram Mor. Multifunctional host defense peptides: antiparasitic activities. *The FEBS journal*, 276(22):6474–6482, 2009.
45. Phasit Charoenkwan, Chanin Nantasenamat, Md Mehedi Hasan, and Watshara Shoombuatong. ittca-hybrid: Improved and robust identification of tumor t cell antigens by utilizing hybrid feature representation. *Analytical biochemistry*, 599:113747, 2020.
46. Hanne B Rasmussen, Sven Branner, Finn C Wiberg, and Nicolai Wagtmann. Crystal structure of human dipeptidyl peptidase iv/cd26 in complex with a substrate analog. *Nature structural biology*, 10(1):19–25, 2003.
47. Yannan Bin, Wei Zhang, Wending Tang, Ruyu Dai, Menglu Li, Qizhi Zhu, and Junfeng Xia. Prediction of neuropeptides from sequence information using ensemble classifier and hybrid features. *Journal of proteome research*, 19(9):3732–3740, 2020.
48. Haibo He and Edwardo A. Garcia. Learning from imbalanced data. *IEEE Transactions on Knowledge and Data Engineering*, 21(9):1263–1284, 2009.
49. Brian W. Matthews. Comparison of the predicted and observed secondary structure of t4 phage lysozyme. *Biochimica et Biophysica Acta (BBA) - Protein Structure*, 405(2):442–451, 1975.
50. Amir Pandi, David Adam, Amir Zare, Van Tuan Trinh, Stefan L Schaefer, Marie Burt, Björn Klabunde, Elizaveta Bobkova, Manish Kushwaha, Yeganeh Foroughijabbari, et al. Cell-free biosynthesis combined with deep learning accelerates de novo-development of antimicrobial peptides. *Nature Communications*, 14(1):7197, 2023.
51. Alba Ledesma-Fernandez, Susana Velasco-Lozano, Javier Santiago-Arcos, Fernando López-Gallego, and Aitziber L Cortajarena. Engineered repeat proteins as scaffolds to assemble multi-enzyme systems for efficient cell-free biosynthesis. *Nature Communications*, 14(1):2587, 2023.

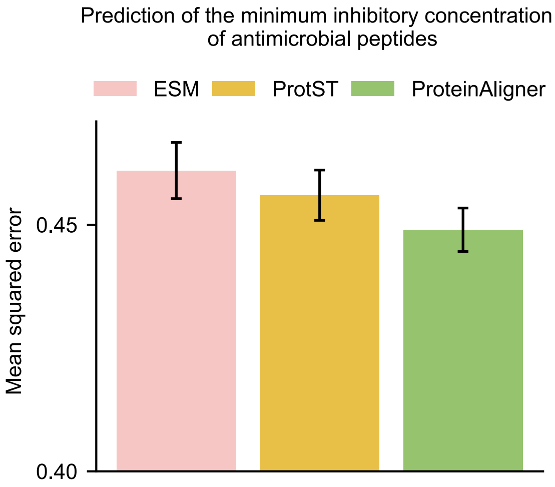

Extended Data Fig. 1 | ProteinAligner surpasses ESM and ProtST in predicting the minimum inhibitory concentration (MIC) of antimicrobial peptides, achieving a lower mean squared error.

Method

Dataset preprocessing. The pretraining data for ProteinAligner was sourced from the UniProtKB/Swiss-Prot (32) and RCSB PDB (33) databases. UniProtKB/Swiss-Prot is a well-curated repository containing high-quality protein sequences across a wide variety of organisms, along with detailed annotations on protein functions and properties. We utilized version UniProt 2023_02, which was released on May 2, 2023. The RCSB PDB database offers a comprehensive collection of experimentally determined 3D protein structures, derived from methods such as X-ray crystallography, nuclear magnetic resonance (NMR) spectroscopy, and cryo-electron microscopy (cryo-EM). It includes protein structures from a wide range of proteins, such as enzymes, receptors, and antibodies, originating from diverse organisms.

From these databases, we collected sequence-text pairs and sequence-structure pairs (Extended Data Fig. 2). The sequence-text pairs were sourced from UniProtKB/Swiss-Prot. We first obtained a collection of protein entries from Swiss-Prot that included textual descriptions of their functions, by filtering for entries where the `commentType` field

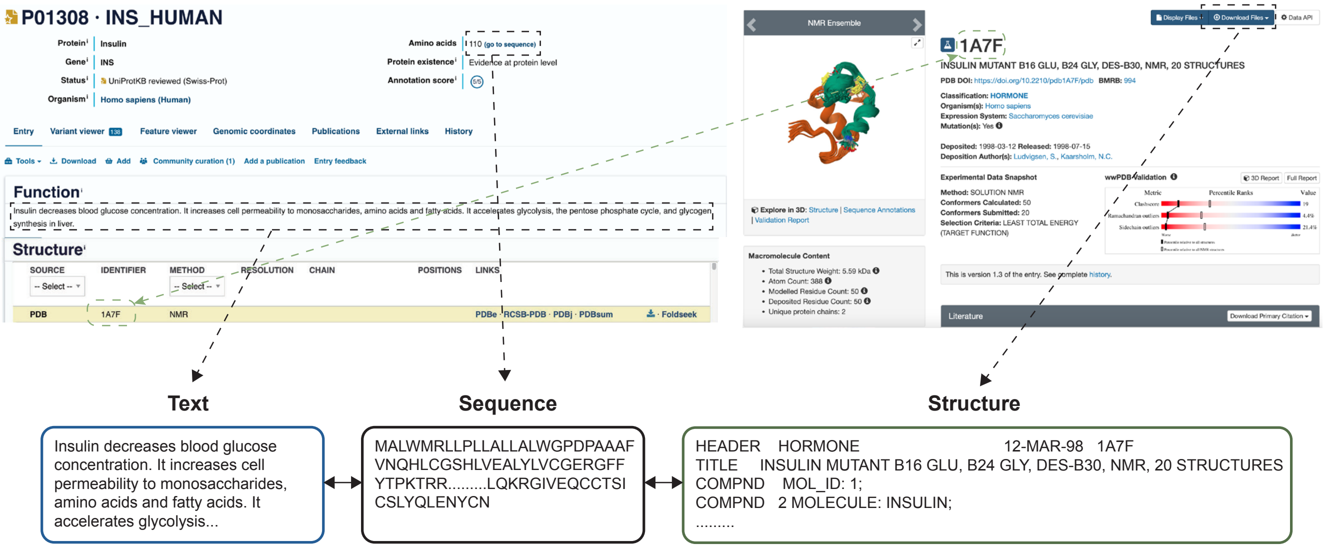

Insulin decreases blood glucose concentration. It increases cell permeability to monosaccharides, amino acids and fatty acids. It accelerates glycolysis, the pentose phosphate cycle, and glycogen synthesis in liver.

Insulin decreases blood glucose concentration. It increases cell permeability to monosaccharides, amino acids and fatty acids. It accelerates glycolysis...

```
MALWMRLLPLLALLALWGPDPAAAF
VNQHLCGSHLVEALYLVCGERGFF
YTPKTRR.........LQKRGIVEQCCTSI
CSLYQLENYCN
```

```
HEADER    HORMONE                              12-MAR-98   1A7F
TITLE     INSULIN MUTANT B16 GLU, B24 GLY, DES-B30, NMR, 20 STRUCTURES
COMPND    MOL_ID: 1;
COMPND   2 MOLECULE: INSULIN;
.........
```

Extended Data Fig. 2 | An illustration of constructing sequence-text and sequence-structure pairs from the UniProtKB/Swiss-Prot and RCSB PDB databases. Sequence-text pairs were generated by linking each protein's amino acid sequence with its functional description, both available on the same UniProtKB/Swiss-Prot webpage. Sequence-structure pairs were created by matching the protein sequences from UniProtKB/Swiss-Prot with their corresponding structures in RCSB PDB, using PDB IDs.

was set to 'Function'. We then retrieved the corresponding sequence for each protein in this collection. Specifically, we accessed the UniProt ID from the `primaryAccession` field and used it to retrieve the corresponding protein FASTA file from the UniProt website, which contains the protein's sequence. We downloaded all available PDB files from the May 2, 2023 dataset release (33), comprising 200,734 experimentally determined protein structures. We then employed the UniProt ID mapping tool[1] to link the structures in the PDB files to their corresponding amino acid sequences in the FASTA files. To address memory constraints during pretraining, we excluded protein sequences longer than 300 residues, yielding 133,726 sequence-structure pairs and 290,480 sequence-text pairs.

Encoders in ProteinAligner. ProteinAligner utilizes ESM (16) to learn representations for protein sequences. ESM, a protein language model, was pretrained on 65 million protein sequences from UniRef50 (52) by predicting masked amino acids. The model features 33 transformer layers and an embedding dimension of 1280, allowing it to effectively capture the complexities inherent in protein sequences. To encode protein structures, ProteinAligner employs ESM-IF1 (9), a model trained to address the inverse folding problem - predicting the amino acid sequence from a protein's backbone atom coordinates. ESM-IF1 comprises an encoder and a decoder, where the encoder extracts a representation vector from the input structure, which is then fed into the decoder to generate the corresponding sequence. ProteinAligner utilizes only the encoder from ESM-IF1, omitting the decoder component. The encoder is composed of four Geometric Vector Perceptron Graph Neural Network (GVP-GNN) (30) layers for geometric feature extraction, followed by eight transformer encoder layers to capture long-range interactions between these features. ESM-IF1 was trained on 12 million AlphaFold2 (8) computed protein structures and 16,000 experimentally verified structures, along with their associated sequences from the UniRef50 dataset (52). The text encoder is a transformer model comprising eight layers and a total of 78 million parameters.

ProteinAligner pretraining. Given a protein sequence S and a protein structure R, we employ the sequence encoder $E_s(\cdot)$ and structure encoder $E_r(\cdot)$ to extract representation vectors $\mathbf{s} = E_s(S)$ and $\mathbf{r} = E_r(R)$ for S and R, respectively. To ensure that the representations are similar when S and R belong to the same protein, and dissimilar when they do not, we minimize the InfoNCE (31) contrastive learning loss:

$$\mathcal{L}_{s,r} = -\log \frac{\exp\left(\mathbf{s}_i^\top \mathbf{r}_i/\tau\right)}{\exp\left(\mathbf{s}_i^\top \mathbf{r}_i/\tau\right) + \sum_{j\neq i} \exp\left(\mathbf{s}_i^\top \mathbf{r}_j/\tau\right)}, \quad \textbf{(1)}$$

where $\mathbf{s}_i$ and $\mathbf{r}_i$ represent the sequence and structure representations of the same protein i, while $\mathbf{s}_i$ and $\mathbf{r}_j$ represent the representations of different proteins i and j. This loss function encourages the alignment of $\mathbf{s}_i$ and $\mathbf{r}_i$ and discourages the similarity between $\mathbf{s}_i$ and $\mathbf{r}_j$. The temperature parameter τ controls the sharpness of the softmax distribution.

Similarly, given a protein sequence S and a protein text description T, we use the sequence encoder $E_s(\cdot)$ and the text encoder $E_t(\cdot)$ to obtain representation vectors $\mathbf{s} = E_s(S)$ and $\mathbf{t} = E_t(T)$ for S and T, respectively. To ensure that the representations are similar when S and T correspond to the same protein, and dissimilar when they

[1] https://www.uniprot.org/id-mapping

do not, we minimize the following InfoNCE contrastive learning loss:

$$\mathcal{L}_{s,t} = -\log \frac{\exp\left(\mathbf{s}_i^{\top}\mathbf{t}_i/\tau\right)}{\exp\left(\mathbf{s}_i^{\top}\mathbf{t}_i/\tau\right)+\sum_{j\neq i}\exp\left(\mathbf{s}_i^{\top}\mathbf{t}_j/\tau\right)}. \quad \textbf{(2)}$$

During pretraining, we minimized the sum of the two loss functions with equal weights. The temperature parameter τ was configured to 0.07. Pretraining was carried out over 20 epochs with total batch size of 80 using 40 A100 GPUs. We optimized the model weights using the AdamW optimizer (53), with an initial learning rate of 5×10^{-6}, weight decay of 1×10^{-4}, and betas of $(0.9, 0.95)$. The learning rate was dynamically adjusted throughout pretraining via the CosineAnnealingLR scheduler (54).

Type I anti-CRISPR activity detection. The overall model architecture for this task is illustrated in Extended Data Fig. 3a. The sequence encoder pretrained by ProteinAligner was fine-tuned using data specific to this task. The classification module was based on a CNN which was composed of two 1D convolutional layers, each with a stride of 1 and a kernel size of 7. The first convolutional layer takes an input of 1280 channels and outputs 4 channels. The second convolutional layer maintains the same input and output dimensions. Batch normalization (55) and ReLU activation (56) are applied after each convolutional layer. Following the convolutional layers, two fully connected layers, each with a hidden size of 4, are employed for final classification.

During training, we optimized model weights using the Adam (57) optimizer with an initial learning rate of 3×10^{-3}, over a maximum of 250 epochs with a batch size of 32. To prevent overfitting, we employed early stopping when the decrease in training loss fell below 0.005 and applied weight decay, starting at 0.01 and gradually reducing to 0.001. We also performed a hyperparameter sweep on the dropout rate (58), exploring values between 0.3 and 0.5. Additionally, we implemented a learning rate reduction strategy, decreasing the rate by a factor of 0.9 if validation performance did not improve for 10 consecutive epochs.

The metrics used to evaluate model performance in this task include accuracy, precision, recall rate, and F1 score. These metrics are calculated based on the number of true positives (TP), false positives (FP), false negatives (FN), and true negatives (TN), and are defined as follows:

$$\begin{aligned}
\text{Accuracy} &= \frac{TP+TN}{TP+TN+FP+FN},\\
\text{Precision} &= \frac{TP}{TP+FP},\\
\text{Recall} &= \frac{TP}{TP+FN},\\
\text{F1 score} &= 2\times\frac{Precision\times Recall}{Precision+Recall}.
\end{aligned} \quad \textbf{(3)}$$

Pathogenic missense variants prediction. The overall model architecture is depicted in Extended Data Fig. 3b. For this task, the sequence encoder pretrained by ProteinAligner was fine-tuned. The classification module was based on a multi-layer perceptron, which comprises a fully connected layer with a hidden state size of 1280, a dropout layer with a probability of 0.5, a leaky ReLU activation (59), and a second fully connected layer with a softmax activation function. We employed the Adam optimizer with a learning rate of 1×10^{-4} and a weight decay of 1×10^{-3}, training the model for a maximum of 200 epochs with a batch size of 32. To mitigate overfitting, we applied an early stopping strategy: if validation performance did not improve over 10 consecutive epochs, training was halted, and the model checkpoint with the best validation performance was retained as the final model. The model's performance was evaluated using accuracy, precision, recall, and F1 score, as defined in Equation 3.

Thermostability prediction. The overall model architecture is depicted in Extended Data Fig. 3c. The structure encoder, pretrained using ProteinAligner, was fine-tuned for this task. The classification module, implemented as a multi-layer perceptron (MLP), includes a fully connected layer with a hidden dimension of 128, followed by layer normalization (60), a ReLU activation, and a second fully connected layer to produce the classification logits. For model optimization, we employed the AdamW (53) optimizer with a learning rate of 2×10^{-2}, a batch size of 4, and a weight decay of 5×10^{-2}. A one-cycle learning rate scheduler (61) was applied, and the model was trained for 8 epochs. Performance was evaluated based on accuracy, precision, recall, and F1 score, as defined in Equation 3.

Identification of potent bioactive peptides. The overall model architecture is illustrated in Extended Data Fig. 3d. The sequence encoder, pretrained by ProteinAligner, was fine-tuned for each of the eight tasks. The classification module employs a convolutional neural network (CNN) with six layers, structured as follows: a 1D convolutional layer (kernel size = 3, stride = 1, padding = 2), followed by BatchNorm and ReLU activation; a max pooling layer (kernel size = 2, padding = 1) and a dropout layer with a probability of 0.15; another 1D convolutional layer (kernel size = 3, stride = 1, padding = 2), followed by BatchNorm and ReLU activation; a max pooling layer (kernel size = 2, padding = 1) and a dropout layer with a probability of 0.15; a fully connected layer with a hidden state size of 64, followed by ReLU activation and a dropout layer (probability = 0.15); and finally, a fully connected binary classification layer with sigmoid activation.

In the blood–brain barrier peptide (BBP) prediction task, the objective is to classify whether a peptide can penetrate the blood–brain barrier (i.e., BBP) (40). We employed the BBPpred dataset (40), consisting of 100

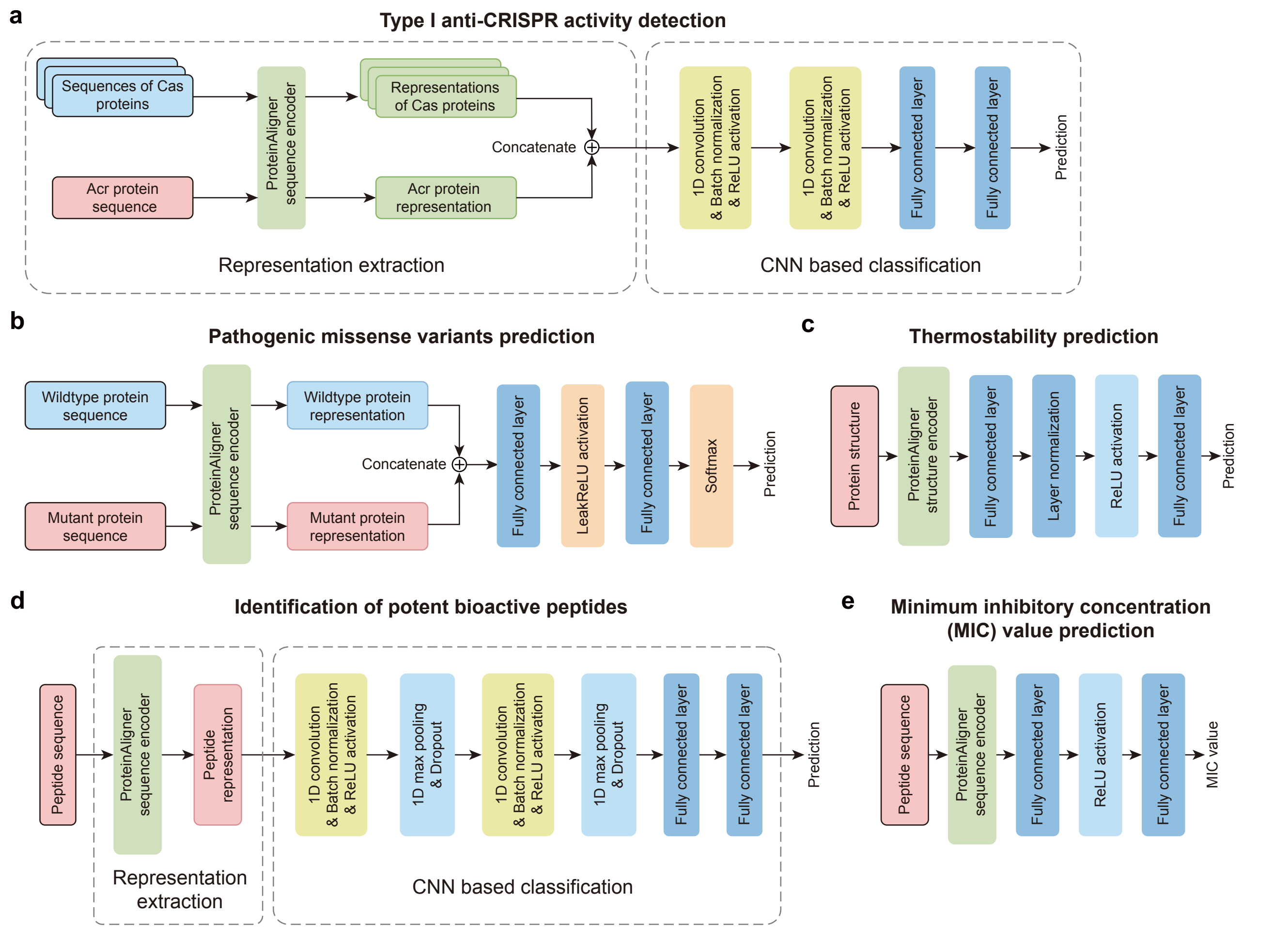
a
Type I anti-CRISPR activity detection
Sequences of Cas proteins
Acr protein sequence
ProteinAligner sequence encoder
Representations of Cas proteins
Acr protein representation
Concatenate
Representation extraction
1D convolution & Batch normalization & ReLU activation
1D convolution & Batch normalization & ReLU activation
Fully connected layer
Fully connected layer
Prediction
CNN based classification
b
Pathogenic missense variants prediction
Wildtype protein sequence
Mutant protein sequence
ProteinAligner sequence encoder
Wildtype protein representation
Mutant protein representation
Concatenate
Fully connected layer
LeakReLU activation
Fully connected layer
Softmax
Prediction
c
Thermostability prediction
Protein structure
ProteinAligner structure encoder
Fully connected layer
Layer normalization
ReLU activation
Fully connected layer
Prediction
d
Identification of potent bioactive peptides
Peptide sequence
ProteinAligner sequence encoder
Peptide representation
Representation extraction
1D convolution & Batch normalization & ReLU activation
1D max pooling & Dropout
1D convolution & Batch normalization & ReLU activation
1D max pooling & Dropout
Fully connected layer
Fully connected layer
Prediction
CNN based classification
e
Minimum inhibitory concentration (MIC) value prediction
Peptide sequence
ProteinAligner sequence encoder
Fully connected layer
ReLU activation
Fully connected layer
MIC value

Extended Data Fig. 3 | Model architectures used in downstream tasks. a, Model architecture used in type I anti-CRISPR activity detection. **b**, Model architecture used in pathogenic missense variants prediction. **c**, Model architecture used in thermostability prediction. **d**, Model architecture used for identifying potent bioactive peptides. **e**, Model architecture used for predicting minimum inhibitory concentration values.

BBPs and 100 non-BBPs for training, and 19 BBPs and 19 non-BBPs for testing. In the umami peptide prediction task, the goal is to determine whether a peptide elicits an umami taste (41). For this task, we used the iUmami-SCM dataset (62), with a training set of 112 umami peptides and 241 non-umami peptides, and a test set of 28 umami peptides and 61 non-umami peptides. In the antioxidant peptide prediction task, the aim is to classify peptides based on their antioxidant properties (42). We used the AnOxPePred dataset (63), containing 582 antioxidative peptides and 241 non-antioxidative peptides for training, with a test set comprising 28 antioxidative peptides and 61 non-antioxidative peptides. For the antiviral peptide prediction task, the objective is to predict whether a peptide has antiviral activity (preventative and therapeutic against viral infections) (43). We utilized the ABPDiscover dataset (64), which includes 2321 antiviral peptides and 2321 non-antiviral peptides for training, and 623 antiviral peptides and 623 non-antiviral peptides for testing. In the antiparasitic peptide prediction task, the goal is to identify peptides with antiparasitic activity (44). Using the PredAPP dataset (65), we trained on 255 antiparasitic peptides and 255 non-antiparasitic peptides, and tested on 46 antiparasitic peptides and 46 non-antiparasitic peptides. The tumor T cell antigen prediction task aims to classify peptides capable of inducing a T-cell immune response (45). We used the iTTCA-Hybrid dataset (45), including 470 antigenic peptides and 318 non-antigenic peptides for training, with 122 antigenic peptides and 75 non-antigenic peptides for testing. For the dipeptidyl peptidase IV (DPP-IV) inhibitory peptide prediction task, the goal is to identify peptides that inhibit DPP-IV activity (66). We used the iDPPIV-SCM dataset (66), containing 532 inhibitory peptides and 532 non-inhibitory peptides for training, and 133 inhibitory peptides and 133 non-inhibitory peptides for testing. Lastly, in the neuropeptide (NP) prediction task, the aim is to classify peptides as neuropeptides or non-neuropeptides (47). We used the PredNeuroP dataset (47), containing 1940 neuropeptides and 1940 non-neuropeptides for training, and 485 neuropeptides and 485 non-neuropeptides for testing.

During training, we optimized the model using stochastic gradient descent (SGD) with a learning rate of 1×10^{-2}, momentum of 0.5, and no weight decay, over 200 epochs. Additionally, we applied step decay for learning rate adjustment and utilized early stopping based on validation accuracy, halting training if no improvement was observed for 40 consecutive epochs. Model performance was assessed using several metrics, including accuracy (ACC), balanced accuracy (BACC) (48), sensitivity (SN), specificity (SP), Matthews correlation coefficient (MCC) (49), and area under the ROC curve (AUC). These metrics were derived from the counts of true positives (TP), false positives (FP), false negatives (FN), and true negatives (TN), and are defined by the following equations:

$$\begin{aligned}
\text{ACC} &= \frac{TP+TN}{TP+TN+FP+FN},\\
\text{SN} &= \frac{TP}{TP+FN},\\
\text{SP} &= \frac{TN}{TN+FP},\\
\text{BACC} &= 0.5 \times \text{SN} + 0.5 \times \text{SP},\\
\text{MCC} &= \frac{(TP \times TN) - (FN \times FP)}{\sqrt{(TP+FN)(TN+FP)(TP+FP)(TN+FN)}}.
\end{aligned} \tag{4}$$

Minimum inhibitory concentration (MIC) value prediction. The model architecture is illustrated in Extended Data Fig. 3e. The sequence encoder, pretrained with ProteinAligner, was fine-tuned to address this task. The classification module is a multi-layer perceptron (MLP) consisting of two fully connected layers, with a hidden size of 256 and a ReLU activation function. We employed the Adam optimizer with an initial learning rate of 1×10^{-4}, training the model for 200 epochs. Throughout the training process, the learning rate was dynamically adjusted at each epoch using the LambdaLR (67) scheduler. To assess the model's performance, we used mean squared error (MSE) as the evaluation metric, defined as:

$$\text{MSE} = \frac{1}{n}\sum_{i=1}^{n}(\hat{y}_i - y_i)^2, \tag{5}$$

where n denotes the number of examples, $\hat{y}_i$ represents the model's prediction for the i-th example, and y_i is the corresponding ground-truth value.

Data availability

The FASTA and PDB datasets are publicly available in UniProtKB Swiss-Prot and RCSB PDB, respectively. The FASTA and PDB entries for protein sequences and structures in the pretraining data, along with their textual descriptions, are available at https://drive.google.com/file/d/1Ff28ajdyUDQl9JtSNQcUz-6Nbz7FXdEA/view?usp=sharing All the data used in downstream tasks is also publicly available. The data used in type I anti-CRISPR activity detection is available at AcrTransAct. The data for predicting the pathogenicity of missense variants is available at VariPred. The data used in thermostability prediction is available at HotProtein. The data used in peptide bioactivity prediction is available at UniDL4BioPep. The data for predicting the minimum inhibitory concentration (MIC) of antimicrobial peptides is available at DeepAMP.

Code availability

The source code for ProteinAligner pretraining, along with the pretrained checkpoints, is available at https://github.com/Alexiland/ProteinAligner Additionally, links to the code for downstream tasks can be found in the README file.

References

52. Baris E Suzek, Yuqi Wang, Hongzhan Huang, Peter B McGarvey, Cathy H Wu, and UniProt Consortium. Uniref clusters: a comprehensive and scalable alternative for improving sequence similarity searches. *Bioinformatics*, 31(6):926–932, 2015.
53. Ilya Loshchilov, Frank Hutter, et al. Fixing weight decay regularization in adam. *arXiv preprint arXiv:1711.05101*, 5, 2017.
54. Ilya Loshchilov and Frank Hutter. Sgdr: Stochastic gradient descent with warm restarts. In *International Conference on Learning Representations*, 2022.
55. Sergey Ioffe and Christian Szegedy. Batch normalization: Accelerating deep network training by reducing internal covariate shift. In *International Conference on Machine Learning*, pages 448–456. PMLR, 2015.
56. Vinod Nair and Geoffrey E Hinton. Rectified linear units improve restricted boltzmann machines. In *International Conference on Machine Learning*, pages 807–814, 2010.
57. Diederik P Kingma. Adam: A method for stochastic optimization. *arXiv preprint arXiv:1412.6980*, 2014.
58. Nitish Srivastava, Geoffrey Hinton, Alex Krizhevsky, Ilya Sutskever, and Ruslan Salakhutdinov. Dropout: A simple way to prevent neural networks from overfitting. *Journal of Machine Learning Research*, 15(56):1929–1958, 2014.
59. Andrew L. Maas, Awni Y. Hannun, and Andrew Y. Ng. Rectifier nonlinearities improve neural network acoustic models. In *International Conference on Machine Learning*, pages 3–8, 2013.
60. Jingjing Xu, Xu Sun, Zhiyuan Zhang, Guangxiang Zhao, and Junyang Lin. Understanding and improving layer normalization. *Advances in neural information processing systems*, 32, 2019.
61. Leslie N. Smith. Super-convergence: Very fast training of neural networks using large learning rates. In *International Conference on Machine Learning (ICML)*, pages 1–10, 2018.
62. Phasit Charoenkwan, Janchai Yana, Chanin Nantasenamat, Md Mehedi Hasan, and Watshara Shoombuatong. iumami-scm: a novel sequence-based predictor for prediction and analysis of umami peptides using a scoring card method with propensity scores of dipeptides. *Journal of Chemical Information and Modeling*, 60(12):6666–6678, 2020.
63. Tobias Hegelund Olsen, Betül Yesiltas, Frederikke Isa Marin, Margarita Pertseva, Pedro J García-Moreno, Simon Gregersen, Michael Toft Overgaard, Charlotte Jacobsen, Ole Lund, Egon Bech Hansen, et al. Anoxpepred: using deep learning for the prediction of antioxidative properties of peptides. *Scientific reports*, 10(1):21471, 2020.
64. Sergio A Pinacho-Castellanos, César R García-Jacas, Michael K Gilson, and Carlos A Brizuela. Alignment-free antimicrobial peptide predictors: improving performance by a thorough analysis of the largest available data set. *Journal of Chemical Information and Modeling*, 61(6):3141–3157, 2021.
65. Wei Zhang, Enhua Xia, Ruyu Dai, Wending Tang, Yannan Bin, and Junfeng Xia. Predapp: predicting anti-parasitic peptides with undersampling and ensemble approaches. *Interdisciplinary Sciences: Computational Life Sciences*, pages 1–11, 2022.
66. Phasit Charoenkwan, Sakawrat Kanthawong, Chanin Nantasenamat, Md Mehedi Hasan, and Watshara Shoombuatong. idppiv-scm: a sequence-based predictor for identifying and analyzing dipeptidyl peptidase iv (dpp-iv) inhibitory peptides using a scoring card method. *Journal of proteome research*, 19(10):4125–4136, 2020.
67. Leslie N. Smith. Cyclical learning rates for training neural networks. In *2017 IEEE Winter Conference on Applications of Computer Vision (WACV)*, pages 464–472. IEEE, 2017.